

High-flip-angle slice-selective Parallel RF Excitation with 8 Channels at 7 Tesla

K. Setsompop¹, V. Alagappan², A. Potthast³, U. Fontius⁴, L. Wald⁵, and E. Adalsteinsson¹

¹EECS, Massachusetts Institute of Technology, Cambridge, ma, United States, ²A. A. Martinos Center for Biomedical Imaging, MGH, Charlestown, ma, United States, ³Siemens Medical Solutions, Charlestown, ma, United States, ⁴Siemens Medical Solutions, Erlangen, Germany, ⁵A. A. Martinos Center for Biomedical Imaging, Department of Radiology, MGH, Charlestown, MA, United States

Introduction At high magnetic field, B_1^+ inhomogeneity causes undesired non-uniformity in SNR and contrast. Parallel RF “spoke”-based 3D trajectory designs have been shown to correct this problem and produce highly uniform in-plane magnetization with excellent slice selection with relatively short excitation durations [1,2]. However, at large flip angles the excitation k-space based design method fails. Recently, several large-flip-angle excitation designs have been proposed [3-8]. In this work we propose and demonstrate large-flip parallel excitation designs for 90° and 180° spin-echo pulses for 8 channels at 7T in the presence of B_1^+ inhomogeneity similar to that seen in human brain *in vivo*.

Theory and Methods

RF design: Powell-based nonlinear iterative optimization with a local cost function [4] was used for the design in combination with the solution from the linear class of large tip angle (LCLTA) design [5] serving as the initial starting point for the iteration. Three-spoke pulses were designed via Magnitude least square (MLS) optimization [9], to achieve improved magnitude profile over conventional least squares at the cost of a smooth spatial phase variation that resulted in negligible intra-voxel dephasing. To satisfy peak RF voltage limitations, the RF pulses were VERSEd, reducing SAR with an acceptable increase in pulse duration. Finally, using the method from [10], B_0 field map was incorporated into the RF design, and the pulses were optimized for increased spectral bandwidth (50 Hz) to provide robustness to field map errors.

Experimental verification: Excitation waveforms for a 90° pulse as well as a 90° - 180° spin echo pulses were designed and implemented for excitations on a water phantom using an 8-channel TX-RX stripline coil array (fig. 1) on a 7T human MRI scanner (Siemens Medical Solutions, Erlangen Germany). The slice thickness of the axial section was 1cm, and all measurements were performed in a 17-cm diameter doped water phantom with cylindrical loading ring used to mimic human coil loading conditions and B_1^+ variations. Fig. 1 illustrates the similarity of the transmit-receive (TX-RX) birdcage image for in-vivo and for the phantom both with peak-to-trough magnitude ratio of approximately 9.

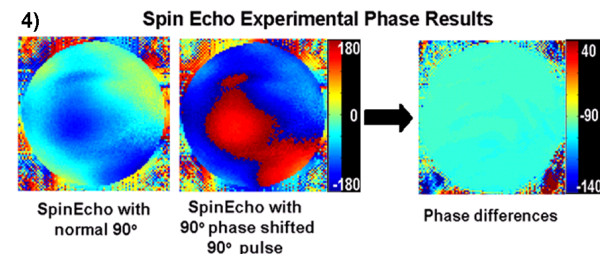
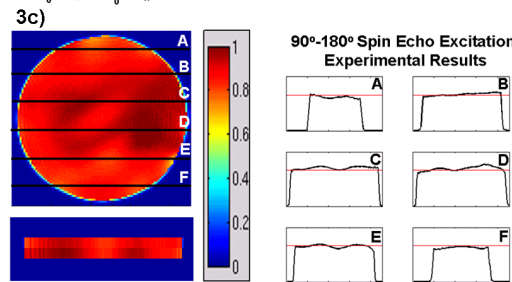
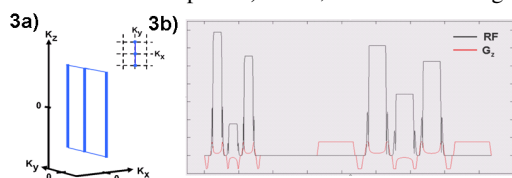
B_1 maps: Quantitative B_1^+ maps (Gauss per Volt) of the 8 transmit channels were obtained by first estimating the birdcage receive profile via transmitting and receiving with the birdcage mode at a set of voltage levels, and using a Simplex search algorithm in Matlab to fit the resulting intensities to the equation:

$$I(x, y) = RX(x, y) \times \frac{[1 - e^{-TR/T_1(x,y)}] \sin \theta(x, y)}{1 - e^{-TR/T_1(x,y)} \cos \theta(x, y)}$$

Once the birdcage receive profile (RX) was obtained, the profile of each

transmit channel was estimated by obtaining a low flip angle image on each channel ($TR=1s \gg T_1=0.165s$) and dividing the image by the birdcage receive profile.

Results and discussion A 90° degree 1-cm thick slice selective excitation was performed using a 3-spoke, 4.4-ms long pTx pulse. Figure 2 demonstrates the excellent in-plane B_1^+ mitigation (top left) and slice selection (bottom left) achieved with this pulse (after division of the image by the estimated RX profile). Also, shown on the right are the excitation profiles at equi-spaced horizontal sections. The flip angle was empirically



verified to be 90° by collecting images with voltages around the predicted optimal setting and observing maximum signal intensity at 90° . **Spin Echo:** The pulse sequence used for the spin-echo ($TE = 20$ ms) is shown in Fig 3b), where a versed 3-spoke design (fig3a) with duration of 3.26 ms and 5.6 ms were used for a 90° 2-cm thick slice selective excitation followed by a 180° 1-cm thick slice selective refocusing pulse, respectively. Shown in red is the G_z gradient, and in black is the RF pulse used in one of the excitation coils. Gradient crushers for the 180° pulse can be seen, along with the effect of the VERSE on the gradient and RF. Figure 3c shows the resulting excitation which exhibits good in-plane profile and slice selection. To check the spin-echo nature of the sequence, an additional experiment was performed whereby a 90° phase shift is added to the 90° RF excitation pulse of the sequence and observing the relative phase difference of the resulting profiles of -90° (fig 4). The final experimental excitation phase of the original and the modified sequence are shown on the left. The phase different between the two is shown on the right with a zoomed in phase scale, showing a -90° degree phase difference throughout the image.

Conclusion: Parallel excitation waveforms for a 90° pulse and a 90° - 180° spin echo pair were designed and validated on a water phantom with large B_1^+ profile variation, similar to that observed in human at 7T. Slice-selective excitations with parallel RF systems offer means to implement conventional high-flip excitation sequences without severe pulse-duration penalty, even at very high B_0 field strengths where large B_1^+ inhomogeneity is present.

Support: NIH R01EB006847, R01EB007942, R01EB000790, and NCRR grant P41RR14075, Siemens Medical Solutions, R.J.Shillman Career Development Award, and the MIND Institute.

References: 1. Setsompop K. et al, MRM 2006:56:1163. 2. Zhang Z. et al, MRM 2006:57:842. 3. Ulloa J.L. et al, ISMRM, p.3016, 2006 4. Setsompop K. et al, ISMRM p.677, 2007 5. Xu D. et al, ISMRM p.1696, 2007 6. Xu D. et al, MRM 2007:58:326 7. Grissom W. et al, ISMRM p.677, 2007 8. Grissom W. et al, ISMRM p.1689, 2007 9. Setsompop K. et al, submitted to ISMRM 2008 10. Setsompop K. et al, submitted to ISMRM 2008

